Global Scientific JOURNALS

GSJ: Volume 8, Issue 8, August 2020, Online: ISSN 2320-9186
www.globalscientificjournal.com

Study of mechanical and corrosion properties for seamless gas pipelines

Ali H. AL-Assadi*, Ahmed Asker, Abdou Abdel- Samad ***, M. Samuel******

*Ali H. AL-Assadi , Iraqi Student production engineering & machine design. Faculty of engineering Mansoura university alialassady5@gmail.com .

** Dr. Ahmed Asker, Mansoura university, Faculty of engineering, Mansoura, Egypt a.askar@mans.edu.eg

*** Prof. Dr. Abdou Abdel –Samed, Mansoura university, Faculty of engineering, Mansoura, Egypt asamad@mans.edu.eg .

****Prof. Dr M. SAMUEL, Mansoura university, Faculty of engineering, Mansoura ,Egypt magdy_s@mans.edu.eg

Abstract

The mechanical and corrosion performances of carbon steel arc weld joints in service environments have been established to be influenced by the process parameters used in carrying out the welding process. Gas Metal Arc Welding (GMAW) and Shielded Metal Arc Welding (SMAW) processes are leading in the development in arc welding process which are higher productivity, common and good in quality . **PURPOSE**: In this study, the effects of different parameters on welding penetration, microstructural , hardness and corrosion resistance measurement in carbon steel by using the gas metal arc welding and shielded metal arc welding are investigated .**MATERIALS AND METHODS**: The variables that choose in this study are weld process, arc voltage, welding current and corrosion environment .The base metal seamless pipe carbon steel grade B that having the 7.1mm thickness of base metal (ASME A106) was used and the arc voltage and welding current were chosen as range (27 – 38) V, and (50 – 100) A of (SMAW) The welding speed was chosen constant as 100 mm/min .The arc voltage and welding current were chosen as range (28 – 34) V, and (130 – 180) A of (GMAW) . The welding speed was chosen constant as 200 mm/min. The penetration, microstructure and micro-hardness were determined with the aid of Vickers micro-hardness tester for each specimen after the welding process and the effect of it was studied. Then studied the effect two corrosion environment on carbon steel. The corrosion of the samples in atmospheric corrosion and soil were investigated using mass loss. **RESULTS**: The weld bead shape varied directly with the welding process. The microstructure of the weld joints consists of δ-ferrite and pearlite phases. The heat input affects the weld joint hardness negatively. The corrosion performance of the weld joints is close to each other however, the performance decreased with the increase in the heat energy input.

Key words: Carbon steel, welding Parameters, soil corrosion, atmospheric corrosion

NTRODUCTION

carbon steel seamless pipes have a wide range of applications because of their excellent engineering properties. These properties include acceptable corrosion resistance, good weldability, formability, high impact and tensile strength. They provide high impact strength and corrosion performance at relatively lower cost compared to other alloys. Carbon steel seamless pipes has good welding characteristics and is suited to all standard welding methods such as shielded metal arc welding

(SMAW), gas tungsten arc welding (GTAW), submerged arc welding (SAW), gas metal arc welding (GMAW) [1] Due to its combination of good mechanical, corrosion properties and cost, carbon steel seamless pipes has found applications in a wide variety of different Industries as conveying water, oil, gas and other fluids , low and medium pressure boiler is used in the manufacturing process of various structural low and medium pressure boiler superheated steam pipes, boiling water pipes and superheated steam, carbon Steel Seamless Pipes has lot of potential to carry huge amount of weigh [1,2].

In view of the fact that arc welding processes like SMAW and GMAW offer a wide spectrum of thermal energy for joining different thicknesses of steel, it was considered important that undertaking the present study would be very beneficial in gaining an understanding of the mechanical properties of low-carbon steel that influence the service performance of the welded joints under different heat input combinations i.e. low heat input and high heat input [3-4]. The chemical composition of steel has impact on the weldability and the mechanical properties of the material. According to Monika et al. [5], several elements are purposefully added in the production of structural steel, but other undesirable elements may equally be present arising from the scrap materials charged during the steelmaking process. Carbon, manganese, tungsten and other elements increase strength and may increase the risk of cold cracking and therefore higher preheat and inter pass temperatures, better hydrogen control and sometimes post heat are necessary to avoid cracking [5]. The heat affected zone (HAZ) is prone to failure due to the possibility of hydrogen induced cracking and only way to weld such steels is to use low hydrogen ferritic steel filler wire [6].

Often, carbon steel parts are joined together using arc welding technique for making sophisticated engineering components and structures. The major issues about arc welding of carbon steel are the large heat affected zone (HAZ) and corrosion damage initiating from the weld joints. According to Karci et al. [7], the heat affected zone refers to that portion of the base metal that has not been melted but the structural or mechanical properties of the metal have been altered by the welding heat. In the past, some work has been done on the arc welding of carbon steel. The arc current has the greatest effects on bead geometry [8]. The heat input effect on the tensile strength, hardness, impact strength and corrosion performances of the welded [9-10-12]. V-grooved edge preparation has better mechanical properties as compared with straight edge preparation under the same conditions [9]. It observed that high heat input, coarse grains appear in the HAZ which resulted in lower hardness values in this zone [10-11]. Selecting appropriate values for process variables is essential in order to control heat-affected zone (HAZ) dimensions and get the required bead size and quality. The welding current, arc voltage, welding speed, heat input rate are hosen.

In recent years, atmospheric corrosion of materials have attracted materials community for it accounts for more failures on both a tonnage basis and cost basis than any other type of environmental corrosion. Tremendous amounts of materials in industries, automobiles, bridges and buildings are exposed to the atmosphere and attacked by pollutant and water.

The results shown that temperature is an important factor in the corrosion rate of carbon steel [13]. The rainfall was the strongest environmental factor influencing the initial atmospheric corrosion rate. Relative humidity significantly influenced the corrosion of carbon steels in low-precipitation environments and non-rainfall period [14]. Fan et al [15] investigated the evolution of the rust layers on carbon steel in high humidity and heat marine atmospheric environment by wet/dry cyclic acceleration corrosion tests in this study .

Failures of buried pipeline systems (water, sewage, oil and gas) due to corrosion are an inevitable concern for owners and asset managers in any country, as they reduce the service life of pipelines. Sudden bursts of pipes and the consequent significant losses. Therefore, understanding factors causing corrosion of buried pipes is necessary.

The major soil properties such as soil resistivity, soil moisture content, soil redox potential, and chloride, sulphate, bicarbonate contents effect on corrosion of low carbon steel pipe in Alkaline Soils [16]. It was revealed that the corrosion rate of pipes buried in soil increases with increase in moisture content up to critical moisture [17-18].

Xianming et al [19] studied the corrosion behavior of X80 pipeline steel weld joints in an acidic red soil solution. The results show that uniform corrosion occurs on the entire surface of the weld joint after 840h immersion. The corrosion degree of heat affected zone (HAZ) is more serious than that of base metal (BM) and weld zone (WZ). The corrosion rate of HAZ specimen is always higher than those of WZ and BM specimens throughout the separated immersion. The accelerating corrosion of HAZ may come from its microstructure change, its corrosion sensitivity and the deterioration of mechanical performance of corrosion product on it.

As welding parameters. Though some work has been reported on the effect of variation of heat input on the hardness and mechanical and corrosion properties of carbon steel seamless pipes. The effect of heat inputs on the corrosion properties of the welded joints has not been well researched in real enviromental. Also, the individual effect of the welding processes and the relative significance of each of the processes on the mechanical and corrosion performance of the electric arc weldments has not been reported. The aim of the research is to investigate the effects of welding processes, parameters and heat energy input on the mechanical performance and corrosion in different environment of the arc weld joints production. Welding processes change the microstructures and properties of surrounding steel and its surface texture. As a result, welded joints are susceptible for both pitting

MATERIALS AND METHODS

Materials

Seamless pipe carbon steel grade B was purchased from an oil company, Cairo, Egypt and is the base material to be used for the research. The chemical composition of the carbon steel grade B as received from the supplier is given in Table 1 according to ASME A106. The microstructure of parent metal Fig.1 is composed of ferrite with small amount of pearlite. The base material was cut into specimens of dimension 60 mm X 40 mm X 7.11mm using hydraulic hacksaw machine. Forty eight (48) of such samples were made. It is noteworthy to state that prior to the welding process, the plates were cleaned and degreased in

order to remove different forms of contaminants. The welding electrode used for the production of the weldment is of specification “AWS A5.1” of (SMAW) and "AWS A5.18"of (GMAW). Table 2 shows the chemical composition of the filler used. This was preferred in order to have an electrode that is suitable for the range of the welding current to be used.

Table 1 Chemical composition (wt.%) of parent metal.

STEEL GRAD	Composition max %								
	C	**Mn**	**P**	**S**	**Cu**	**Ni**	**Cr**	**Mo**	**Si**	**V**
GR B	0.30	0.29 to 1.0(	0.035	0.035	0.4	0.4	0.4	0.15	0.10	0.08

Table 2 Chemical composition requirement for weld metal

AWS classification	Weight percent								
	C	**Mn**	**Si**	**P**	**S**	**Ni**	**Cr**	**Mo**	**V**	Combined limit for Mi+Ni+Cr+Mo+V
E6010	0.2	1.2	1.00	N.S.	N.S.	0.30	0.2	0.3	0.08	N.S.
E7018	0.15	1.6	0.75	0.035	0.035	0.30	0.2	0.3	0.08	1.75
ER70S-6	0.15	1.85	1.15	0.025	0.035	0.15	0.15	0.15	0.03	**Cu**=0.5

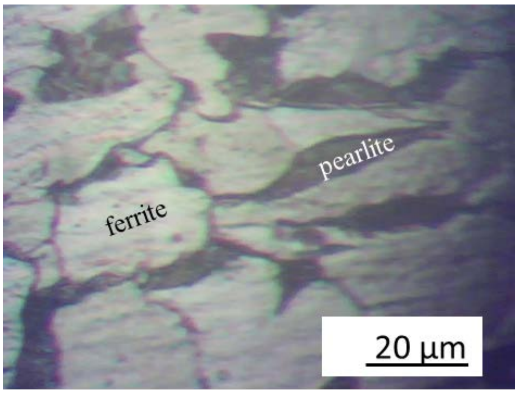

Fig. 1. Micrographs of parent metal.

Welding Process

The arc welding process was performed at the the Central Metallurgical Research and Development Institute, Helwan (CMRDI). All standard welding procedures was adhered to. After some trial experiments were done. (Fig. 2(a) and (b)) shows the electric arc welding process.

The current and voltage of welding were varied while the speed was kept constant of each weld process. Prior to each welding process, a root gap of 2 mm was allowed between the metal plates to be joined together so as ensure high quality weld with deep penetration. heat input per unit length of weld (H) for each combination of the parameters were calculated using equation 1 according to AWS D1.5. H is the heat input per unit length of weld (KJ/mm).

$$H = \frac{I \times V \times 0.06}{S} \quad (1)$$

Where: - I is current (AMP), V is voltage(V) and S is travel speed (mm/min) . Each carbon steel weldment was made in two passes. As shown in Fig. 2 (c), each pass commenced from the same side of the plate identified as the welding start point (Start) and a cooling time of 2 min was allowed in between the successive passes. Weldments were produced at different welding parameters giving eight (8) welding conditions, as presented in Table 3. six different weldments were done at each welding condition so as ensure the valid ability and reliability of the results obtained.

All samples were believed that it takes few seconds for welding process to be stable. All weld samples were ground. Samples formed at high, medium and low heat input were selected and examined for microstructural changes using optical microscope.

Table 3 SMA and GMA welding conditions and parameters

process	pass	electrode	Diam (mm)	I(A)	V(V)	S(mm/min)	H(KJ/mm)
SMAW1	Root pass	E6010	2.5	50	34	100	1.02
	Fill pass	E7018	2.5	80	27	100	1.296
SMAW2	Root pass	E6010	2.5	60	38	100	1.368
	Fill pass	E7018	2.5	100	27	100	1.62
GMAW1	Root pass	ER70S-6	0.8	130	34	200	1.326
	Fill pass	ER70S-6	0.8	160	30	200	1.44
GMAW2	Root pass	ER70S-6	0.8	160	30	200	1.44
	Fill pass	ER70S-6	0.8	180	28	200	1.512

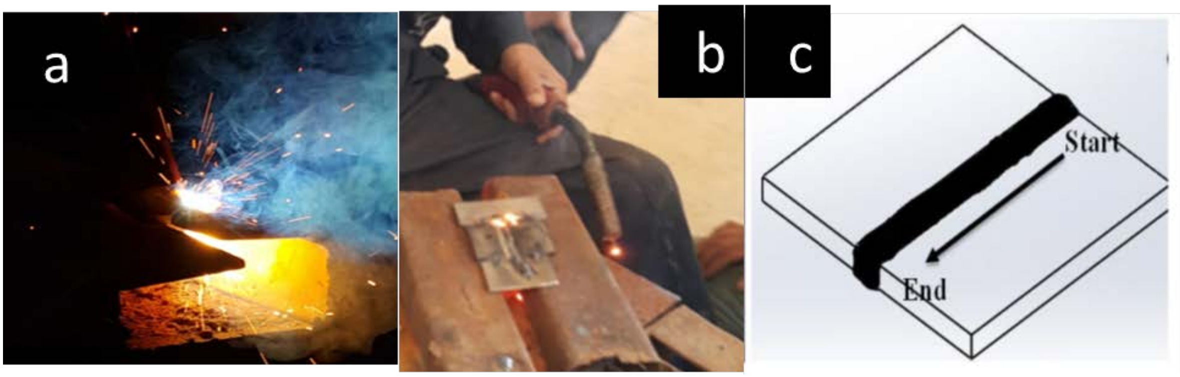

Fig. 2. (a) and (b) A picture showing the electric arc welding of the carbon steel plates and (c) a schematic describing the welding direction

Microstructure

In order to observe the micro-structural changes that take place during welding, corresponding to each heat input combination; specimens were machined out from the weld pads. After polishing and macro etching the cross sections of the joints were captured with the help of image software coupled with a stereo zoom microscope at a magnification of 50 X to facilitate measuring of the details like cross sectional areas of the fusion zone and HAZ. Standard polishing procedures were used for general micro-structural observations. Microstructures of different zones of interest like weld metal, HAZ and fusion boundary under different heat input combinations were viewed and captured with an optical microscope (TENA) coupled with an image software.

Micro-Hardness Test

Micro-hardness test was carried out on all the weldment samples formed using Vickers hardness tester. The indentations were made using a 9.8 N load and a dwell time of 10s.

Corrosion Test

To evaluate surface layer for the four different welded joint samples, in two different environment and Visual inspection and mass loss test were done. The samples were cut into 6 cm x 8 cm to give it an exposed area of 48 cm2. Thereafter, samples were ground so as to reduce variations in the microstructures of the samples' top surfaces. then coated on all sides except the top surface

At Atmospheric corrosion, to simulate the real atmosphere environment the climate chamber is used (Fig 3), where acidic rain and humidity atmosphere attack the samples. acidic rain and humidity atmosphere mainly come from add the calculated quantities of diluted hydrochloric acid to water for the duration of the test to maintain PH 5.5 at 45˚C and aeration .

At soil corrosion, to simulate the real underground environment the samples buried into plastic containers of 500x400x500 mm dimensions and non-reactive to acidic chemicals and the soil with specimens buried in them. The soil(clay) was prepared and sieved to avoid any variation in corrosion results due to different particle sizes and consequent variation in aeration, in the containers following uniform compaction to maintain a uniform density throughout the container. and select the moisture content required

Duration of the test is about 53 days; each period a weight change (ΔW) was estimated. Finally, the change in the weight was plotted versus time. Visual inspection was done to investigate the surface layer attack and the formed corrosion product.

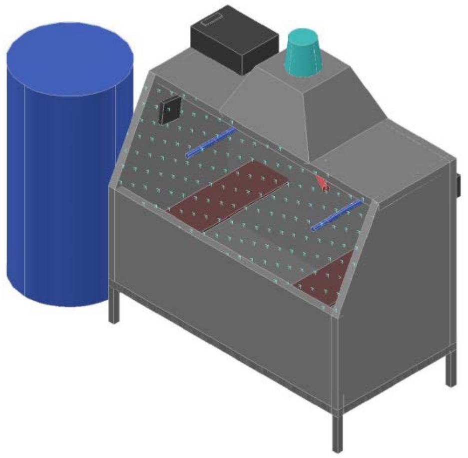

Fig 3 . climate chamber.

RESULTS AND DISCUSSION

Welding Quality

The suitable welding current for the samples was firstly established to be within the range of 50–100 A for SMAW and the range of 130-180 A for GMAW. observed at GMAW process that high spatter, high deposit, high quality weld surface and faster than SMAW process. Also, observed at SMAW process higher penetration than GMAW process. Fig.4. presents the pictures of some quality weld obtained within the chosen process. This indicates that these processes suitable for weld carbon steel pipe even though, the differences in the cost and experience welder

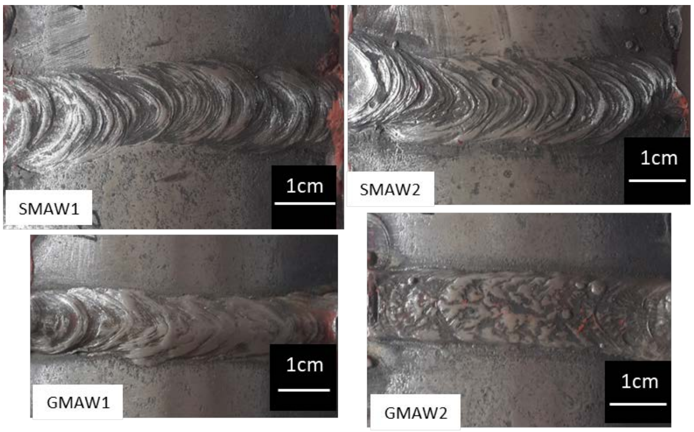

Fig. 4. Pictures of the electric arc weldments of carbon steel obtained

Microstructure

The optical micrographs of the weld center line (WCL), coarse grain heat affected zone (CGHAZ) and fine grain heat affected zone (FGHAZ) of the four weld samples made at variety heat energy per unit weld length are presented in Fig.5. It was observed that weld joints were void cracks and visible pores. This is evidence that all weldments made within the process were of good quality the weld zone for the four selected samples are presented in Fig.5. The images reveal two prominent phases which are (1) a continuous grey-like and (2) black region phase. Similar observation has been reported in the past by Bailey (1984). [20]. The continuous grey-like and black region phase were identified as delta (δ) ferrite and pearlite phase respectively. As seen in the Fig.5, the δ ferrite phase appears to be of lower number density in the weld sample obtained at low heat input when compared with the weld sample formed at high heat input. These microstructural changes have been shown in Fig.5. The changes in (gas metal arc welding and shielded metal arc welding) parameters are influence the effect of the microstructure of weld metal. The increased welding current, welding speed and arc voltage the grain size of microstructure also different from one point to another point. The Fig.(5j) and (5i)) below shown at SMAW2 with higher heat input, the large grain boundaries have shown but at SMAW1 with lower heat input, the grain boundaries become smallest. According Bodude & Momohjimoh [9] the formation of perlite is believed to be beneficial to the corrosion and mechanical performance of the weldment. However, the delta ferrite has been proved to be a softer phase and is undesirable in the weld.

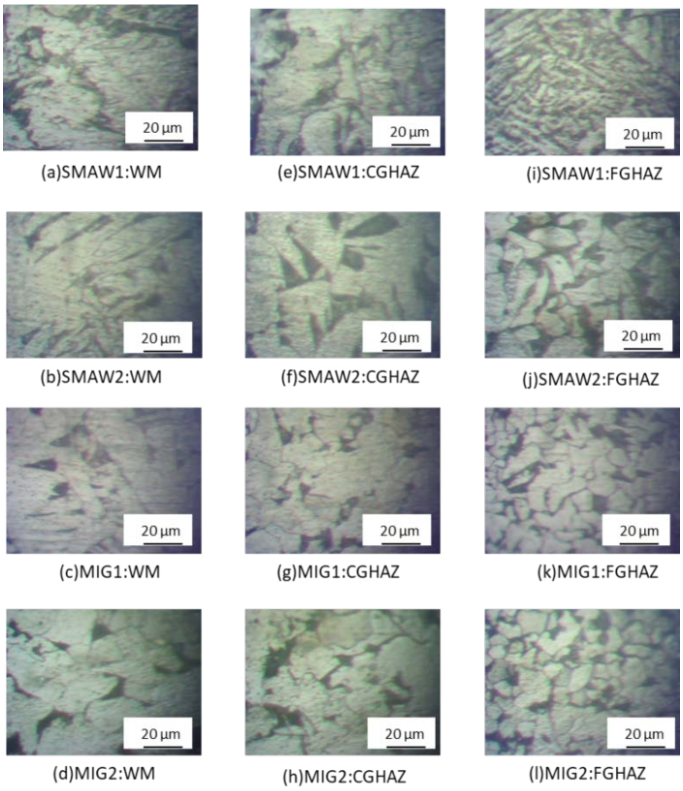

Fig. 5. Optical micrographs of various regions of welded steel joints.

Micro - hardness measurements

Forty measurements were made vertically to the weld axis in two different heights of micro-hardness measurements were performed from the weld root (1/3 and 2/3 height) of each weld joints. The distance between two different imprints of every penetrator measurement were performed every 1 mm, in order to avoid the interference among the measurements, but also to ensure that the measurements are close enough to report the variations in micro-hardness. Each value presented is an average of randomly chosen of three samples for each group. The results were approved according to the statistical analysis of the date was carried out using IBM SPSS Statistics 26. The statistical test applied is the two-way mixed ANCOVA.

The same are shown in Fig. 6. Figure also shows that the micro hardness , it is observed that as the indent or traverses outwards (parallel to the base plate surface) from the center of the weld/fusion zone towards the fusion boundary, micro hardness increases with decrease in heat input from 181.8 HV to 207.6 HV for low heat input and 168.9 HV to 178 HV for high heat input welded joint around HAZ region. Which is due to the fact that cooling rate is relatively higher at the area adjoining the base metal

In all the joints, HAZ area adjacent to the fusion boundary was coarse grained HAZ (CGHAZ) which possessed low hardness whereas the HAZ area adjacent to the base metal was fine grained HAZ (FGHAZ) which possessed high hardness. The reason for this trend of micro hardness in the HAZ of all the joints is that the area adjacent to the weld/fusion zone experiences relatively slow cooling rate and hence has coarse grained microstructure, whereas the area adjoining the base metal undergoes high cooling rate due to steeper thermal gradients and consequently has fine grained microstructure. This is evident from the trend depicted by the micro hardness profile within the HAZ of each of these joints. In general it is observed from these micro hardness studies that hardness follows an increasing trend in the order of weld metal, HAZ, unaffected base metal and fusion boundary for all the joints made at different heat inputs. It is also observed that there is significant grain coarsening in the HAZs of all the joints. Further it is observed from the optical micrographs. shown that the extent of grain coarsening in the HAZ increases with increase in heat input Fig. 5

Rise in the micro hardness with value of 182 HV, 175 HV and 169 HV respectively for low, medium and high heat input as shown in Fig. 6. High hardness as possessed by the fusion boundary zone (FBZ) in all the joints can be attributed to the presence of partially unmelted grains at the fusion boundary which are partially adopted as nuclei by the new precipitating phase of the weld metal during the solidification stage. After reaching this peak value micro hardness shows a decreasing trend in the HAZ.

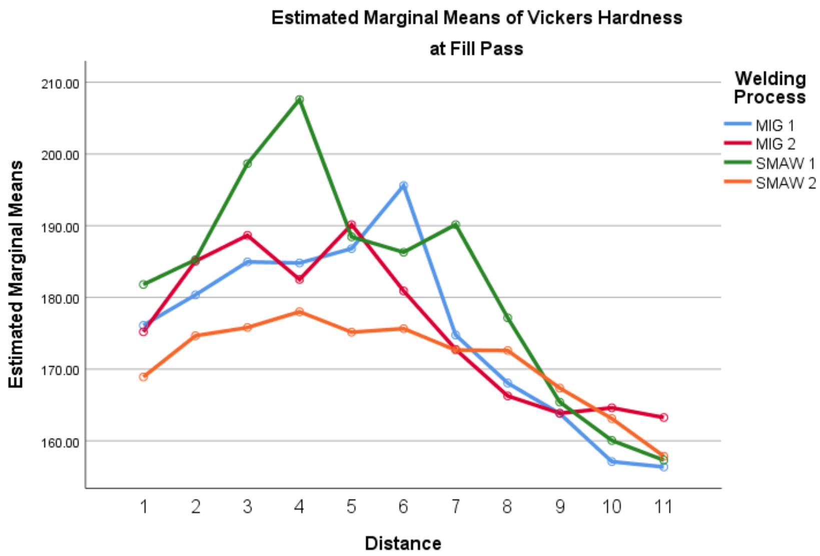

Fig.6 Comparison between the micro-hardness at different points of the weldments at different heat inputs

Also, it was observed that the hardness in the GMAW2 increases more than SMAW2 even though there is a slight heat input difference. In GMAW1 process, the energy density is comparatively higher than that in SMAW1 process. The wider arc column is also a reason for this wide FBZ (Fig.7 (a)). This is due to the fact that the high self-quenching rates that are associated with GMAW process certainly promote the fast cooling rates due do not have covered by slag. This could be attributed to this narrow FBZ (Fig.7 (c)).

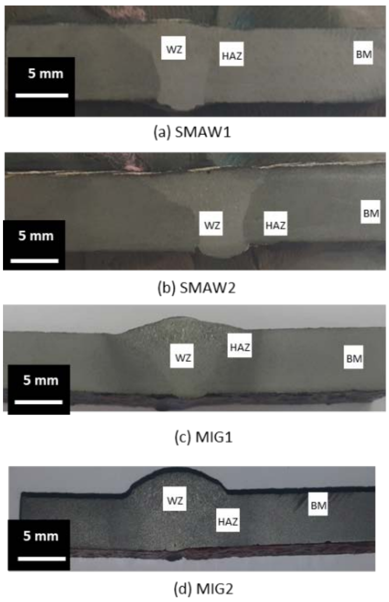

Fig. 7. Pictures of weld cross-section

Also, the formation of the δ ferrite phases after solidification partially contributed to the weaker surface observed in the weld joints. The decreasing hardness with the increasing heat energy per unit length of weld is due to increased heat energy dissipation and slower cooling rate or solidification of the molten metal at the weld zone. The result is in agreement with the past findings of Abioye and Oyetunji et al. [12,19]. The increasing δ ferrite content with increasing heat energy per unit weld length would have contributed to the decreased hardness observed at higher heat energy input.

Corrosion Test

The corrosion rate curve for four selected weld samples obtained at weld processes, current and voltage variation in two enviromental medium are presented in the Fig. 8 .The result revealed that the corrosion performances of the weldments are close each other. The results were approved according to the statistical analysis of the date was carried out using IBM SPSS Statistics 26. The statistical test applied is the three-way mixed ANOVA. The result is in agreement with the past findings of Abioye and Oyetunji et al. [12,19].

The results showed that there a significant effect of the environmental medium on the corrosion rate.

As the corrosion rate in atmospheric more than soil. There was a significant main effect of measurement day on the corrosion rate in atmospheric Contrast shows that there is a significant difference between the data measure in the 28th day and the 38th day. Whereas there was no significant difference between the data measure.

In 38th and the 53rd day. The corrosion rate for the arc weldments (in atmospheric) obined at 1.02 KJ/mm, 1.326 KJ/mm,1.368 KJ/mm and 1.44 KJ/mm are 2.048, 2.131, 2.272 and 2.368 mm/year respectively. The corrosion rate for the arc weldments (in soil) obined at 1.02 KJ/mm, 1.326 KJ/mm,1.368 KJ/mm and 1.44 KJ/mm are 0.530, 0.509, 0.533 and 0.549 mm/year respectively. This shows that the corrosion performance of the weldments decreases as the heat energy input increases. The reason can be traced to the increasing amount of δ-ferrite in the weld samples as the heat energy input increased. The presence of δ-ferrite in the weld metals has been established to be detrimental to their corrosion performance.

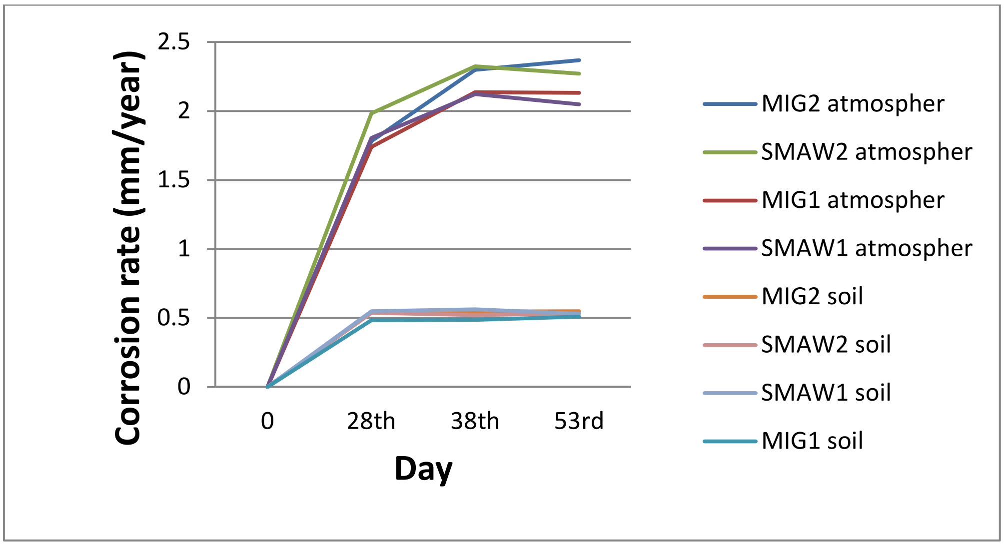

Fig.8 corrosion rate at different enviromental medium of the weldments at different heat inputs

CONCLUSION

In this investigation, an attempt was made to study the effects of welding processes by evaluating the weld joint microstructure, micro-hardness and corrosion resistance of carbon steel seamless pipe joints. welding procedure specification applied in oil companies were employed to weld specimens. From this experimental results; the following important conclusions are derived:

1- The weld bead shape varied directly with the welding process
2- High quality weld joints that are free of visible pores and cracks were produced within the processes utilised in this work.
3- The microstructure of the weld joints consists of δ-ferrite and pearlite phases. The number density of the δ-ferrite in the weld joint microstructure increased with the heat energy per unit weld length.
4- The increase in heat input affects the micro-constituents of base metal, and heat affected zone (HAZ). The heat input affects the weld joint hardness negatively.
5- In all the joints, HAZ area adjacent to the fusion boundary was coarse grained HAZ which possessed low hardness whereas the HAZ area

adjacent to the base metal was fine grained HAZ which possessed high hardness. It is also observed that there is significant grain coarsening in the HAZs of all the joints. Further it is observed from the optical micrographs that the extent of grain coarsening in the HAZ increases with increase in heat input.

6- The corrosion performance of the weld joints is close to each other however, the performance decreased with the increase in the heat energy input.

REFERENCES

1- Davis, J. R. (Ed.). (2006). Corrosion of weldments. ASM international.

2- Papavinasam, S. (2013). Corrosion control in the oil and gas industry. Elsevier

3- Muthupandi, V., Srinivasan, P. B., Seshadri, S. K., & Sundaresan, S. (2003). Effect of weld metal chemistry and heat input on the structure and properties of duplex stainless steel welds. Materials Science and Engineering: A, 358(1-2), 9-16.

4- Ogundimu, E. O., Akinlabi, E. T., & Erinosho, M. F. (2018). Study on microstructure and mechanical properties of 304 stainless steel joints by TIG–MIG hybrid welding. Surface Review and Letters, 25(01), 1850042.

5- Monika, K., Bala Chennaiah, M., Nanda Kumar, P., & Prahalada Rao, P. (2013). The effect of heat input on the mechanical properties of MIG welded dissimilar joints. International Journal of Engineering Research & Technology, 2(9), 1406-1413.

6- Magudeeswaran, G., Balasubramanian, V., Reddy, G. M., & Balasubramanian, T. S. (2008). Effect of welding processes and consumables on tensile and impact properties of high strength quenched and tempered steel joints. Journal of Iron and Steel Research International, 15(6), 87-94.

7- Karcı, F., Kacar, R., & Gündüz, S. (2009). The effect of process parameter on the properties of spot welded cold deformed AISI304 grade austenitic stainless steel. Journal of Materials Processing Technology, 209(8), 4011-4019.

8- Kim, I. S., Son, J. S., Kim, I. G., Kim, J. Y., & Kim, O. S. (2003). A study on relationship between process variables and bead penetration for robotic CO2 arc welding. Journal of Materials Processing Technology, 136(1-3), 139-145.

9- Bodude, M. A., & Momohjimoh, I. (2015). Studies on effects of welding parameters on the mechanical properties of welded low-carbon steel. Journal of Minerals and Materials Characterization and Engineering, 3(03), 142.

10- Boob, A. N., & Gattani, G. K. (2013). Study on Effect of Manual Metal Arc Welding Process Parameters on Width of Heat Affected Zone (Haz) For MS 1005 Steel‖. International Journal of Modern Engineering Research (IJMER), 3(3), 1493-1500.

11- Gharibshahiyan, E., Raouf, A. H., Parvin, N., & Rahimian, M. (2011). The effect of microstructure on hardness and toughness of low carbon welded steel using inert gas welding. Materials & Design, 32(4), 2042-2048.

12- Abioye, T. E. (2017). The effect of heat input on the mechanical and corrosion properties of AISI 304 electric arc weldments. Current Journal of Applied Science and Technology, 1-10.

13- Yin, Z. F., Feng, Y. R., Zhao, W. Z., Bai, Z. Q., & Lin, G. F. (2009). Effect of temperature on CO2 corrosion of carbon steel. Surface and Interface Analysis: An International Journal devoted to the development and application of techniques for the analysis of surfaces, interfaces and thin films, 41(6), 517-523.

14- Pei, Z., Cheng, X., Yang, X., Li, Q., Xia, C., Zhang, D., & Li, X. (2020). Understanding environmental impacts on initial atmospheric corrosion based on corrosion monitoring sensors. Journal of Materials Science & Technology.

15- Fan, Y., Liu, W., Li, S., Chowwanonthapunya, T., Wongpat, B., Zhao, Y., ... & Li, X. (2020). Evolution of rust layers on carbon steel and weathering steel in high humidity and heat marine atmospheric corrosion. Journal of Materials Science & Technology, 39, 190-199.

16- Bansode, V. M., Vagge, S. T., & Kolekar, A. B. (2015). Relationship between Soil Properties and Corrosion of Steel Pipe in Alkaline Soils. Int. J. Res. Sci. Innov, 2(11), 57-61.

17- Wasim, M., & Shoaib, S. (2019). Influence of Chemical Properties of Soil on the Corrosion Morphology of Carbon Steel Pipes. In Metals in Soil-Contamination and Remediation. IntechOpen.

18- Ismail, A. I. M., & El-Shamy, A. M. (2009). Engineering behaviour of soil materials on the corrosion of mild steel. Applied clay science, 42(3-4), 356-362

19- Oyetunji, A., Kutelu, B. J., & Akinola, A. O. (2013). Effects of Welding Speeds and Power Inputs on the Hardness Property of Type 304L Austenitic Stainless Steel Heat-Affected Zone (HAZ). Journal of Metallurgical Engineering (ME) Volume, 2(4).

20- Bailey, A. R. (1984). Introductory Practical Metallography: A Basic Course of Microstructures with 37 Specimens.